ORIGINAL PAPER

RJME
Romanian Journal of Morphology & Embryology
http://www.rjme.ro/

Whole-genome DASL gene expression profiling of hepatocellular carcinoma sub-populations isolated by laser microdissection on formalin-fixed and paraffin-embedded liver tissue samples

CORINA GABRIELA COTOI[1,2)], SHIRIN ELIZABETH KHORSANDI[2)], I. E. PLEŞEA[1)], A. QUAGLIA[2)]

[1)]*Department of Pathology, University of Medicine and Pharmacy of Craiova, Romania*

[2)]*Institute of Liver Studies, King's College Hospital, London, UK*

Abstract

In the last ten years, a multitude of studies focusing on gene expression profiling have attempted to shed light on the molecular and genomic mechanisms leading to hepatocarcinogenesis. One of the downsides of the technology available until recently was that it was limited to RNA extracted from fresh/frozen tissue or cell cultures. Recent advances have made it possible to obtain good quality RNA from formalin-fixed paraffin-embedded (FFPE) tissue, allowing access to a virtually limitless archival resource to be available for retrospective and long-term prospective clinico-pathological studies. Laser-capture microdissection allows the isolation of specific cell populations or of specific microscopic areas of interest from tissue samples. This allows the selective evaluation of gene expression of targeted cell clusters, especially in a very heterogeneous environment as the malignant tissue. In our study, we demonstrated that by laser microdissecting the areas of interest from FFPE tissue we could obtain gene expression signals by running the purified RNA through the Whole Genome DASL assay. A large number of genes were expressed in both subpopulations of hepatocellular carcinoma (classical HCC and cholangiocellular differentiation) as well as in the cirrhotic and non-cirrhotic liver background.

Keywords: liver, formalin-fixed paraffin-embedded tissue, laser microdissection, whole genome DASL assay.

Introduction

Liver carcinogenesis is known to be a multistep process, and hepatocellular carcinoma arises from cumulative genetic and epigenetic alterations [1]. Data from microarray analysis have shown different genetic profiles depending on the etiology of the underlying liver disease or whether HCC originates in non-cirrhotic liver [2]. In the last ten years, a multitude of studies focusing on gene expression profiling have attempted to shed light on the molecular and genomic mechanisms leading to liver carcinogenesis [3].

One of the downsides of the technology available until recently was that it was limited to RNA extracted from fresh/frozen tissue or cell cultures. Recent advances have made it possible to obtain good quality RNA from formalin-fixed paraffin-embedded (FFPE) tissue, allowing access to a virtually limitless archival resource to be available for retrospective and long-term prospective clinicopathological studies.

The Illumina Inc. specially designed gene expression profiling method DASL (cDNA-mediated Annealing, Selection, Extension and Ligation), has been developed for the analysis of fragmented RNA samples [4–6]. The WG-DASL assay is based on the original DASL assay [7], but differs by having a significant increase in the number of transcripts assayed in parallel, while keeping the essential ability of analyzing degraded samples [4].

Laser-capture microdissection allows the isolation of specific cell populations [8] or of specific microscopic areas of interest from tissue samples. This allows the selective evaluation of gene expression of targeted cell clusters [9], especially in a very heterogeneous environment as the malignant tissue. The successful use of this technique in cancer research [10] and other fields [11–13] and on various types of liver tissues and conditions including hepatocellular carcinoma [14], cholangiocarcinoma [15], primary biliary cirrhosis [16], and liver with chronic hepatitis B and C [17] makes it a very useful adjuvant tool for molecular studies.

In the current study, we have purified RNA from 63 laser capture microdissection samples of subpopulations of hepatocellular carcinoma and non-neoplastic liver obtained from FFPE liver tissue and analyzed it using the Whole-Genome DASL (WG-DASL) assay for gene profile expression.

Materials and Methods

We retrieved from the archive in the Histopathology

Laboratory, Institute of Liver Studies, King's College Hospital, London, UK, 20 cases of hepatocellular carcinoma (HCC) which underwent transplantation or resection between 2008 and 2010.

Livers removed at transplantation were received fresh, and sliced into parallel sections at approximately 1 cm intervals. The livers were re-examined after formalin fixation, and tumors were sampled for routine histological interpretation. Formalin-fixed tissue was embedded in paraffin, and the sections were stained with Hematoxylin and Eosin (HE). All the HCCs examined in this study had microscopic foci of viable hepatocellular carcinomas. The background liver, in sections away from the tumors was also examined.

Additional FFPE sections were cut at 5 μm thickness and placed onto RNase free polyethylene naphthalate (PEN) membrane coated slides and laser microdissected using a Leica LMD 6000 microscope. The Leica LMD 6000 system runs morphometry software, which allowed the instantaneous calculation in μm^2 of the selected areas for microdissection. Areas of classical HCC, cholangiocellular differentiation and background liver were identified and around 10.500.000 μm^2 were microdissected in multiple cuts under low magnification. Microdissected tissue was collected in 1.5 mL microfuge caps (Table 1).

Table 1 – ***Areas of classical HCC, cholangiocellular differentiation and background liver identified and microdissected***

Case No.	Tube No.	Microdissected tissue	Quantity [μm^2]
1.	*1.1*	Cholangiocellular differentiation	12.668.138
	1.2	Hepatocellular carcinoma	10.970.793
	1.3	Background liver	10.410.208
2.	*2.1*	Hepatocellular carcinoma	10.103.144
	2.2	Cholangiocellular differentiation	10.890.359
	2.3	Background liver	10.130.200
3.	*3.1*	Hepatocellular carcinoma 1	10.470.536
	3.2	Hepatocellular carcinoma 2	11.300.523
	3.3	Background liver	10.675.294
	3.4	Hepatocellular carcinoma 3	11.806.367
	3.5	Hepatocellular carcinoma 4	10.391.298
4.	*4.1*	Hepatocellular carcinoma 1	10.123.766
	4.2	Hepatocellular carcinoma 2	10.215.119
	4.3	Hepatocellular carcinoma 3	10.410.454
	4.4	Background liver	11.031.517
5.	*5.1*	Hepatocellular carcinoma 1	11.845.390
	5.2	Hepatocellular carcinoma 2	10.466.194
	5.3	Background liver	11.096.974
6.	*6.1*	Hepatocellular carcinoma 1	11.159.387
	6.2	Cholangiocellular differentiation	10.646.777
	6.3	Hepatocellular carcinoma 2	10.126.662
	6.4	Background liver	10.499.814
7.	*7.1*	Hepatocellular carcinoma 1	10.394.660
	7.2	Hepatocellular carcinoma 2	10.463.303
	7.3	Background liver	10.582.374
8.	*8.1*	Hepatocellular carcinoma	10.245.660
	8.2	Cholangiocellular differentiation	10.415.363
	8.3	Background liver	10.120.255
9.	*9.1*	Hepatocellular carcinoma	10.529.029
	9.2	Background liver	10.441.850
10.	*10.1*	Hepatocellular carcinoma	10.285.114
	10.2	Background liver	11.457.859
11.	*11.1*	Hepatocellular carcinoma	10.868.809
	11.2	Background liver	10.851.756
12.	*12.1*	Atypical tubules	9.030.649
	12.2	Background liver	10.279.754
13.	*13.1*	Hepatocellular carcinoma	11.109.647
	13.2	Background liver	10.489.717
14.	*14.1*	Hepatocellular carcinoma (WD)	10.132.512
	14.2	Hepatocellular carcinoma (PD)	10.100.675
	14.3	Background liver	10 173 969
15.	*15.1*	Hepatocellular carcinoma 1	10.199.063
	15.2	Hepatocellular carcinoma 2	10.419.381
	15.3	Hepatocellular carcinoma 3	10.208.711
	15.4	Hepatocellular carcinoma 4	10.634.786
	15.5	Hepatocellular carcinoma 5	10.711.477
	15.6	Hepatocellular carcinoma 6	10.498.495
	15.7	Background liver	10.169.478
16.	*16.1*	Hepatocellular carcinoma 1	10.044.781
	16.2	Hepatocellular carcinoma 2	12.306.671
	16.3	Hepatocellular carcinoma 3	10.106.879
	16.4	Hepatocellular carcinoma 4	10.274.369
	16.5	Cholangiocellular differentiation	11.300.770
	16.6	Background liver	11.300.770
17.	*A*	Background liver	10.020.583
	B	Hepatocellular carcinoma	11.071.871
18.	*C*	Hepatocellular carcinoma	10.000.000
	D	Background liver	11.014.084
19.	*E*	Cholangiocellular differentiation	11.459.005
	F	Hepatocellular carcinoma	11.517.305
	G	Background liver	11.599.565
20.	*H*	Cholangiocellular differentiation	11.104.526
	A1	Background liver	10.326.776
	B1	Hepatocellular carcinoma	10.057.524

The next step was to purify total RNA from the microdissected formalin-fixed, paraffin-embedded tissue (FFPE) sections using the QIAGEN RNeasy® FFPE Kit for purification of total RNA (Cat. No. 73504), following the protocol set by the manufacturer.

In the beginning of the process all paraffin was removed from the FFPE tissue sections by treatment with xylene. One hundred percent ethanol was then added to extract any residual xylene from the sample. Next, samples were incubated in an optimized lysis buffer, which contained proteinase K, to release RNA from the sections. A short incubation at a higher temperature partially reversed formalin cross-linking of the released nucleic acids, improving RNA yield and quality. The DNase treatment that followed was designed to eliminate all genomic DNA, including very small fragments that could have been present in FFPE samples. Next, the lysate was mixed with Buffer RBC. Appropriate binding conditions for RNA were created by adding ethanol. The sample was then transferred to an RNeasy MinElute spin column, which contained a membrane for binding total RNA, contaminants being efficiently washed away. RNA was then eluted in 14 μL of RNase-free water.

The concentration of the purified RNA was

determined using a NanoDrop spectrophotometer (Nano Drop Technologies; Wilmington, DE) by measuring the absorbance at 260 nm (A260). An absorbance of 1 unit at 260 nm corresponds to 40 µg of RNA per ml (A260 = 1 = 40 µg/mL). The ratio of the readings at 260 nm and 280 nm (A260/A280) provides an estimate of the purity of RNA with respect to contaminants that absorb in the UV, such as protein. Pure RNA has an A260/A280 ratio of 1.8–2.0. The average RNA concentration was 42.3 ng/µL (range: 5.4–178.1) with an average 260:280 ratio of 1.95 (range: 1.66–2.21).

Purified total RNA samples were stored at -80^{0}C until needed for quality control (QC) analysis and gene expression profiling. The QC was done with the help of Qubit® Quantitation Platform and Agilent 2100 Bioanalyzer, representing fluorescence-based and an electrophoretic assay respectively.

Qubit® Quantitation Platform was used based on its highly sensitive fluorescence-based assays. Because the Quant-iT™ assay kit used dyes that are selective for RNA, contaminants in the sample should not affect the quantitation.

The electrophoretic assays were run using the Agilent 2100 Bioanalyzer and the data was interpreted with the help of 2100 expert software. The electrophoretic assays are based on the principles of traditional gel electrophoresis, but a chip format is being used. Every chip is composed from several wells for the samples and the gel and one well for an external standard (ladder). When the wells and channels are filled, the electrodes are connected to a power supply and the chip acts as an integrated electrical circuit. The voltage gradient electrophoretically drives the charged RNA biomolecules, smaller fragments migrating faster than larger ones. In this way, the molecules are separated by size. As dye, molecules intercalate into the RNA strands, these complexes can be detected by laser-induced fluorescence. In this way, data is translated into band images and electropherograms. The integrity of the total RNA sample is determined with the help of the ribosomal ratio and the RNA integrity number (RIN). Numbers from '1' to '10' are used to label the samples, '10' meaning no degradation products and '1' being assigned for a completely degraded sample.

Table 2 shows the data from the spectrophotometry analysis, fluorescence-based Qubit® Quantitation and Agilent 2100 Bioanalyzer electrophoretic assays.

Table 2 – ***Data from spectrophotometry analysis, fluorescence-based quantitation and electrophoresis***

Sample No.	Used in WG-DASL assay	Concentration spectrophotometer [ng/µL]	A260/A280 ratio	Concentration of RNA – Qubit [ng/µL]	Concentration Bioanalyzer [ng/µL]
1.	*No*	4.8	1.98	65.4	2
2.	*No*	1.7	5.52	<20	1
3.	*No*	5.5	1.76	57.1	3
4.	*Yes*	47.5	2.21	219	48
5.	*Yes*	49.3	2.17	250	137
6.	*Yes*	72.3	2.11	392	57
7.	*Yes*	44.9	1.93	211	85
8.	*No*	26.6	1.74	<20	3
9.	*Yes*	76.7	1.9	94.7	16
10.	*Yes*	39.6	1.7	108	24
11.	*Yes*	39.2	1.75	114	34
12.	*Yes*	42.8	1.82	148	30
13.	*Yes*	21.3	1.89	163	7
14.	*Yes*	33.4	1.84	194	29
15.	*Yes*	34.9	1.85	246	11
16.	*Yes*	19.8	1.83	87.1	13
17.	*Yes*	31.6	1.82	198	58
18.	*Yes*	37.2	1.83	205	49
19.	*Yes*	23.6	1.89	107	74
20.	*Yes*	51	1.91	250	19
21.	*No*	15.2	1.66	<20	8
22.	*Yes*	17.4	1.97	95.4	26
23.	*Yes*	16.9	2.17	107	13
24.	*Yes*	37.3	2.11	289	41
25.	*Yes*	49.9	2.06	349	59
26.	*Yes*	15.9	1.98	31.9	9
27.	*Yes*	29.5	2.09	188	45
28.	*Yes*	49.3	2.09	341	125
29.	*Yes*	38.2	2.08	180	52
30.	*Yes*	21.3	2.02	128	25
31.	*Yes*	15.7	2	78.2	16
32.	*Yes*	10.6	1.83	37.2	9
33.	*Yes*	5.4	1.98	21	6
34.	*Yes*	27.9	2.03	152	50

Sample No.	Used in WG-DASL assay	Concentration spectrophotometer [ng/μL]	A260/A280 ratio	Concentration of RNA – Qubit [ng/μL]	Concentration Bioanalyzer [ng/μL]
35.	*Yes*	33.4	1.98	160	26
36.	*No*	4	2.09	22	4
37.	*No*	7.3	1.88	29.8	16
38.	*Yes*	6.1	2.06	37.7	5
39.	*Yes*	33.4	2.1	207	75
40.	*Yes*	42.3	2	250	34
41.	*Yes*	37.5	2.07	265	29
42.	*Yes*	52.3	1.78	201	24
43.	*Yes*	28.4	2.09	138	24
44.	*Yes*	6.7	1.76	31.4	3
45.	*Yes*	32.6	1.95	180	21
46.	*Yes*	57.8	1.86	246	100
47.	*Yes*	38	1.9	159	30
48.	*Yes*	32.4	1.93	122	16
49.	*Yes*	26.7	2.02	168	21
50.	*Yes*	30.9	1.92	161	14
51.	*Yes*	34.4	2.1	272	45
52.	*Yes*	23.7	2.13	200	26
53.	*Yes*	50.1	1.86	243	29
54.	*Yes*	42.6	1.99	277	77
55.	*Yes*	30.4	1.87	176	19

In the next step, the samples were processed at their maximum concentration according to the Illumina Whole-Genome Gene Expression DASL HT Assay Guide (LSN-X-SF & WS-035), using the WG-DASL HT Assay Profiling Reagent Kit.

The WG-DASL assay started by converting through reverse transcription reaction the total RNA into cDNA. This reaction used biotinylated oligo-dT18 and random primers. The biotinylated cDNA was annealed with assay-specific oligonucleotides (ASO) specially designed for a single contiguous 50 nucleotide sequence on each cDNA. These oligonucleotides are composed of two parts: an upstream-specific oligonucleotide (USO) containing a 3' gene-specific sequence and a 5' universal PCR primer, and a downstream-specific oligonucleotide (DSO) containing a 5' gene-specific sequence and a 3' universal PCR primer [7]. The gene-specific sequence corresponds to a capture sequence on the bead chip. A number of 47 000 oligonucleotide pairs (probes) were used, derived from the *National Center for Biotechnology Information Reference Sequence Database* (Build 36.2, Release 38). The ASOs were then annealed to the biotinylated cDNAs and the mixture was bound to Streptavidin-conjugated paramagnetic particles for selection of the cDNA/oligo complexes. Polymerase extension of the USO and ligation to the corresponding DSO followed. The resulting products were PCR-amplified and labeled with a universal fluorescently labeled primer. The single-stranded labeled products were then hybridized on the complementary gene-specific sequence bead to Illumina Whole-Genome Gene Expression Human HT-12 v4 BeadChips and scanned with the iScan™ Reader.

The iScan™ reader includes red and green lasers to detect fluorescence information on the bead chips. The bead chips scan generated intensity data files (**.idat* files) for each sample, each file containing raw intensity data values for every bead in the scanned image. Each bead chip in addition to the probes designed to interrogate the majority of protein coding transcripts had a large set of positive and negative control probes. The Illumina iScan™ software (ICS version 3.2) was used to extract and normalize the expression data (fluorescence intensities) for the mean intensity of all arrays.

The GenomeStudio™ Gene Expression Module v1.0 was used to analyze gene expression data using the intensity file from the scanned microarray images generated by the iScan™ System. This software could be used for gene analysis to quantify gene expression or for differential gene expression analysis to determine the probability of gene expression levels to have changed between two groups or samples. This software averages values for each gene across samples and algorithms automatically use replicates to provide estimates of relative mRNA abundance to detect differential gene expression. In brief, the following were applied to identify differentially expressed genes: a detection *p*-value <0.01 and a differential score >13 (corresponding to a *p*-value <0.05) under the Benjamini and Hochberg False Discovery Rate correction for multiple tests.

Results

According to the RIN label ascribed by the Agilent 2100 Bioanalyzer electrophoretic assay for every sample, the purified RNA from the FFPE was almost entirely degraded. Only 10% of all the samples had a RIN between 2 and 2.6, while 47% and 15 % of them had a RIN between 1 and 2 or equal to 1 respectively. For 28% of the extracted RNA, a RIN value could not be calculated.

Figure 1 shows one "gel-like" image provided by the Agilent 2100 Bioanalyzer and Figures 2 and 3 show the electropherograms for a "good" and "bad" RIN-labeled RNA sample compared to the label (Figure 4).

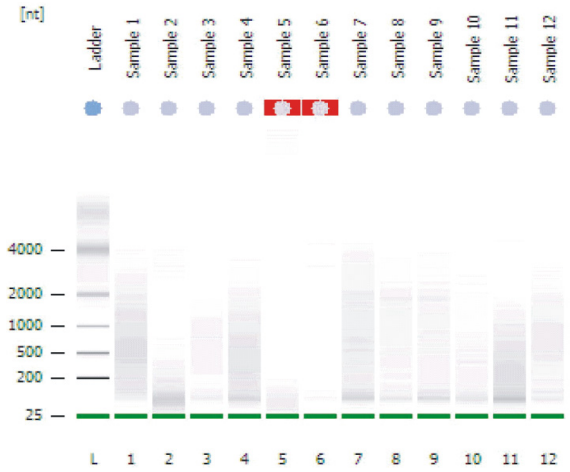

Figure 1 – ***"Gel-like" image provided by the Agilent 2100 Bioanalyzer for the first 12 samples.***

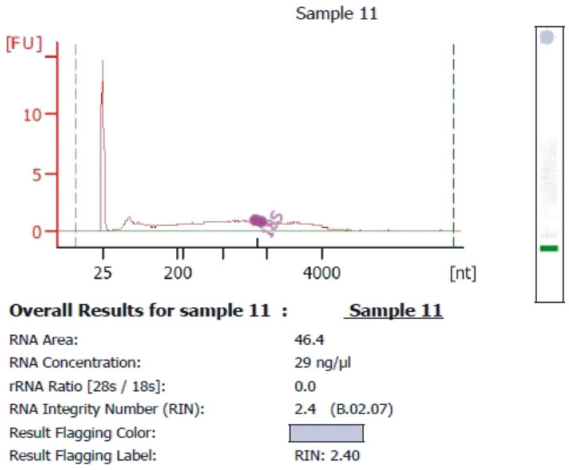

Figure 2 – ***Electropherogram provided by the Agilent 2100 Bioanalyzer showing a "good" RIN-labeled RNA sample.***

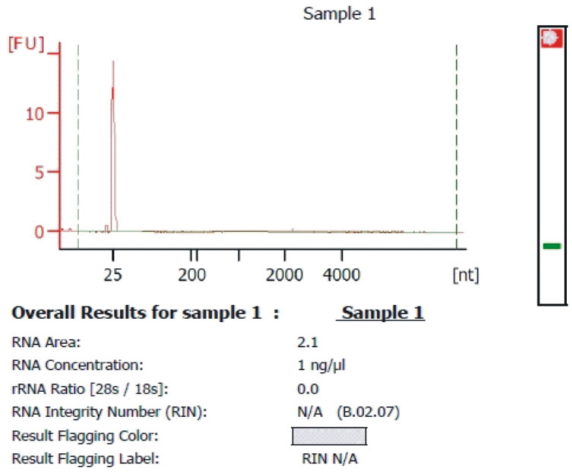

Figure 3 – ***Electropherogram provided by the Agilent 2100 Bioanalyzer showing a "bad" RIN-labeled RNA sample.***

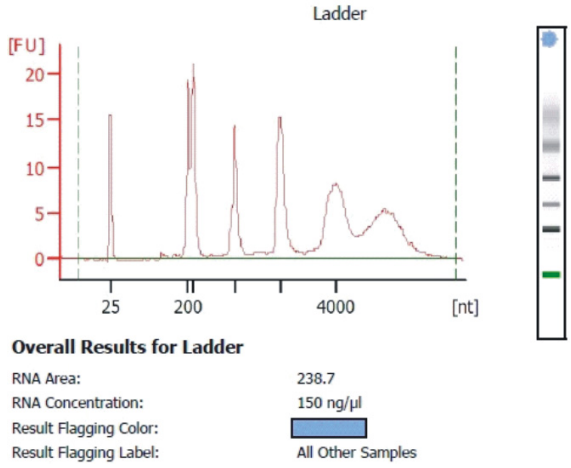

Figure 4 – ***Electropherogram provided by the Agilent 2100 Bioanalyzer for the external standard (ladder).***

After the QC assessment, seven of the samples were excluded from the WG-DASL assay, mostly based on the very low RNA concentration.

A very large number of expressed genes were detected through the WG DASL assay, for both sub-populations of HCC as well as for the background liver (data not shown). For illustrating purposes, we present a differential analysis between the gene expression profile of the classical subpopulation of hepatocellular carcinoma and the gene expression profile of the background liver. The differential analysis highlighted 77 genes that were shown to be significantly different between the gene expression profile of the classical subpopulation of hepatocellular carcinoma and the gene expression profile of the background liver. A total number of 60 genes were down-regulated in HCC when compared to the gene expression profile of the surrounding liver, while 17 genes were shown to be up-regulated.

Table 3 shows the differentially expressed genes between HCC and the background liver, including average signal for the two groups, *p*-values and differential scores.

Table 3 – ***Down-regulated and up-regulated genes in HCC compared to background liver***

Down-regulated genes in HCC compared to background liver							
Gene symbol	***Background liver avg. signal value***	***Background liver detection p-value***	***Background liver differential score***	***HCC avg. signal value***	***HCC detection p-value***	***HCC differential score***	***Gene definition***
CLEC4G	9111	0	0	740.5	0	-58.048	*Homo sapiens* C-type lectin superfamily 4, member G (CLEC4G), mRNA.
VIPR1	33207	0	0	7636.3	0	-42.074	*Homo sapiens* vasoactive intestinal peptide receptor 1 (VIPR1), mRNA.
MARCO	3970.1	0	0	486.5	0	-40.382	*Homo sapiens* macrophage receptor with collagenous structure (MARCO), mRNA.

Down-regulated genes in HCC compared to background liver							
Gene symbol	***Background liver avg. signal value***	***Background liver detection p-value***	***Background liver differential score***	***HCC avg. signal value***	***HCC detection p-value***	***HCC differential score***	***Gene definition***
ACAA2	15004.3	0	0	9196.5	0	-40.149	*Homo sapiens* acetyl-Coenzyme A acyltransferase 2 (mitochondrial 3-oxoacyl-Coenzyme A thiolase) (ACAA2), nuclear gene encoding mitochondrial protein, mRNA.
COLEC10	5085.5	0	0	642.5	0	-28.641	*Homo sapiens* collectin subfamily member 10 (C-type lectin) (COLEC10), mRNA.
FCN3	15615.6	0	0	7255.2	0	-26.504	*Homo sapiens* ficolin (collagen/fibrinogen domain containing) 3 (Hakata antigen) (FCN3), transcript variant 2, mRNA.
APOF	15999	0	0	7048.7	0	-23.357	*Homo sapiens* apolipoprotein F (APOF), mRNA.
BHMT	22961.6	0	0	13508.1	0	-23.357	*Homo sapiens* betaine-homocysteine methyltransferase (BHMT), mRNA.
FBP1	22303.2	0	0	12365.1	0	-22.361	*Homo sapiens* fructose-1,6-bisphosphatase 1 (FBP1), mRNA.
DNASE1L3	11679.7	0	0	3754.1	0	-21.196	*Homo sapiens* deoxyribonuclease I-like 3 (DNASE1L3), mRNA.
FCN2	6235.2	0.0643	0	703.5	0.38055	-20.205	*Homo sapiens* ficolin (collagen/fibrinogen domain containing lectin) 2 (hucolin) (FCN2), transcript variant SV0, mRNA.
CETP	5118.3	0	0	1675.8	0	-20.121	*Homo sapiens* cholesteryl ester transfer protein, plasma (CETP), mRNA.
GHR	20714.4	0	0	13506.8	0	-19.587	*Homo sapiens* growth hormone receptor (GHR), mRNA.
GLS2	2203.2	0	0	621.5	0	-19.245	*Homo sapiens* glutaminase 2 (liver, mitochondrial) (GLS2), nuclear gene encoding mitochondrial protein, mRNA.
ASS1	9466.6	0	0	5323.1	0	-19.233	*Homo sapiens* argininosuccinate synthetase 1 (ASS1), transcript variant 1, mRNA.
ASPG	8152.2	0	0	2987.9	0	-18.79	*Homo sapiens* asparaginase homolog (S. cerevisiae) (ASPG), mRNA.
C6	14369.1	0	0	9531.6	0	-18.329	*Homo sapiens* complement component 6 (C6), mRNA.
CXCL14	2333.1	0	0	346.4	0	-18.221	*Homo sapiens* chemokine (C-X-C motif) ligand 14 (CXCL14), mRNA.
BTG2	3135.8	0	0	1394.4	0	-18.004	*Homo sapiens* BTG family, member 2 (BTG2), mRNA.
IGFBP3	8478.2	0	0	3499.4	0	-17.942	*Homo sapiens* insulin-like growth factor binding protein 3 (IGFBP3), transcript variant 2, mRNA.
STAB2	4322.5	0	0	614.6	0	-17.922	*Homo sapiens* stabilin 2 (STAB2), mRNA.
DUSP1	13708.9	0	0	9170.9	0	-17.638	*Homo sapiens* dual specificity phosphatase 1 (DUSP1), mRNA.
DBH	13651.5	0	0	2395.6	0	-17.441	*Homo sapiens* dopamine beta-hydroxylase (dopamine beta-monooxygenase) (DBH), mRNA.
ATOH8	4010.2	0	0	763.1	0	-17.277	*Homo sapiens* atonal homolog 8 (Drosophila) (ATOH8), mRNA.
THRSP	14320	0	0	7588.3	0	-17.277	*Homo sapiens* thyroid hormone responsive (SPOT14 homolog, rat) (THRSP), mRNA.
APOA5	3499.2	0	0	1586.1	0	-17.094	*Homo sapiens* apolipoprotein A-V (APOA5), mRNA.
CDA	16023.1	0	0	9620.6	0	-17.094	*Homo sapiens* cytidine deaminase (CDA), mRNA.
CFP	2514	0	0	387.1	0	-17.094	*Homo sapiens* complement factor properdin (CFP), mRNA.
GCGR	20931.2	0	0	11120.6	0	-17.094	*Homo sapiens* glucagon receptor (GCGR), mRNA.
TMEM27	2898.3	0	0	635.8	0	-17.094	*Homo sapiens* transmembrane protein 27 (TMEM27), mRNA.

Down-regulated genes in HCC compared to background liver							
Gene symbol	***Background liver avg. signal value***	***Background liver detection p-value***	***Background liver differential score***	***HCC avg. signal value***	***HCC detection p-value***	***HCC differential score***	***Gene definition***
VSIG2	3483.3	0	0	964.9	0	-17.094	*Homo sapiens* V-set and immunoglobulin domain containing 2 (VSIG2), mRNA.
SLC38A2	19367.6	0	0	16926.2	0	-17.04	*Homo sapiens* solute carrier family 38, member 2 (SLC38A2), mRNA.
F9	18059.8	0	0	10952.4	0	-16.885	*Homo sapiens* coagulation factor IX (plasma thromboplastic component, Christmas disease, hemophilia B) (F9), mRNA.
GADD45B	12516.8	0	0	8229.7	0	-16.885	*Homo sapiens* growth arrest and DNA-damage-inducible, beta (GADD45B), mRNA.
HAMP	14538.3	0	0	3726.4	0	-16.885	*Homo sapiens* hepcidin antimicrobial peptide (HAMP), mRNA.
MT2A	20924	0	0	14187.5	0	-16.885	*Homo sapiens* metallothionein 2A (MT2A), mRNA.
RSPO3	1665.6	0	0	223.5	0	-16.885	*Homo sapiens* R-spondin 3 homolog (*Xenopus laevis*) (RSPO3), mRNA.
TF	20973.9	0	0	15763.8	0	-16.885	*Homo sapiens* transferrin (TF), mRNA.
ABCA8	6185.2	0	0	3188.1	0	-16.176	*Homo sapiens* ATP-binding cassette, sub-family A (ABC1), member 8 (ABCA8), mRNA.
NDRG2	4739.3	0	0	2214.7	0	-16.013	*Homo sapiens* NDRG family member 2 (NDRG2), transcript variant 6, mRNA.
ANXA10	2500	0	0	921.3	0	-15.943	*Homo sapiens* annexin A10 (ANXA10), mRNA.
ACAD11	7427.8	0	0	4098.4	0	-15.571	*Homo sapiens* acyl-Coenzyme A dehydrogenase family, member 11 (ACAD11), mRNA.
ATF5	3296.8	0	0	1742.5	0	-15.563	*Homo sapiens* activating transcription factor 5 (ATF5), mRNA.
SRD5A2	2470.1	0	0	678.3	0	-15.563	*Homo sapiens* steroid-5-alpha-reductase, alpha polypeptide 2 (3-oxo-5 alpha-steroid delta 4-dehydrogenase alpha 2) (SRD5A2), mRNA.
HSD17B13	4642.6	0	0	1086.1	0	-15.532	*Homo sapiens* hydroxysteroid (17-beta) dehydrogenase 13 (HSD17B13), mRNA.
ADRA1A	2886.8	0.00005	0	770.4	0.00005	-15.413	*Homo sapiens* adrenergic, alpha-1A-, receptor (ADRA1A), transcript variant 4, mRNA.
FAM65C	7210.6	0	0	1961.9	0	-15.16	*Homo sapiens* family with sequence similarity 65, member C (FAM65C), mRNA.
MYH10	12269.9	0	0	8851.8	0	-14.837	*Homo sapiens* myosin, heavy chain 10, non-muscle (MYH10), mRNA.
C6orf114	2113.7	0	0	923.3	0	-14.824	*Homo sapiens* chromosome 6 open reading frame 114 (C6orf114), mRNA.
SPRYD4	19943	0	0	15328.6	0	-14.61	*Homo sapiens* SPRY domain containing 4 (SPRYD4), mRNA.
ADH1B	17288.1	0	0	12736.1	0	-14.527	*Homo sapiens* alcohol dehydrogenase IB (class I), beta polypeptide (ADH1B), mRNA.
PPP1R3B	5828.9	0	0	3070.8	0	-14.478	*Homo sapiens* protein phosphatase 1, regulatory (inhibitor) subunit 3B (PPP1R3B), mRNA.
ALDH8A1	4557.9	0	0	2310.8	0	-14.304	*Homo sapiens* aldehyde dehydrogenase 8 family, member A1 (ALDH8A1), transcript variant 1, mRNA.
ALDOB	34200.6	0	0	27628	0	-14.075	*Homo sapiens* aldolase B, fructose-bisphosphate (ALDOB), mRNA.
SLC17A2	10741.5	0	0	7231.9	0	-13.856	*Homo sapiens* solute carrier family 17 (sodium phosphate), member 2 (SLC17A2), mRNA.
SMAD6	4074.5	0	0	2185	0	-13.786	*Homo sapiens* SMAD family member 6 (SMAD6), transcript variant 1, mRNA.

Down-regulated genes in HCC compared to background liver							
Gene symbol	***Background liver avg. signal value***	***Background liver detection p-value***	***Background liver differential score***	***HCC avg. signal value***	***HCC detection p-value***	***HCC differential score***	***Gene definition***
FAM180A	623	0	0	47.7	0	-13.669	*Homo sapiens* family with sequence similarity 180, member A (FAM180A), mRNA.
RNF165	12959.8	0	0	6281.5	0	-13.664	*Homo sapiens* ring finger protein 165 (RNF165), mRNA.
ITLN1	2001.4	0	0	28.7	0	-13.657	*Homo sapiens* intelectin 1 (galactofuranose binding) (ITLN1), mRNA.
MAP2K1	4313.1	0	0	2681.2	0	-13.232	*Homo sapiens* mitogen-activated protein kinase kinase 1 (MAP2K1), mRNA.
Up-regulated genes in HCC compared to background liver							
Gene symbol	***Background liver avg. signal value***	***Background liver detection p-value***	***Background liver differential score***	***HCC avg. signal value***	***HCC detection p-value***	***HCC differential score***	***Gene definition***
UBD	5875.8	0	0	13649.6	0	22.073	*Homo sapiens* ubiquitin D (UBD), mRNA.
DGKQ	708	0	0	1746.5	0	17.094	*Homo sapiens* diacylglycerol kinase, theta 110kDa (DGKQ), mRNA.
ALG1L	1355.6	0	0	5662.8	0	16.885	*Homo sapiens* asparagine-linked glycosylation 1-like (ALG1L), mRNA.
CELSR3	637.2	0	0	3011.8	0	16.885	*Homo sapiens* cadherin, EGF LAG seven-pass G-type receptor 3 (flamingo homolog, *Drosophila*) (CELSR3), mRNA.
INTS8	5294.4	0	0	8064.5	0	16.885	*Homo sapiens* integrator complex subunit 8 (INTS8), mRNA.
SLC25A39	25349.1	0	0	29300.6	0	16.885	*Homo sapiens* solute carrier family 25, member 39 (SLC25A39), mRNA.
ADCK2	3827	0	0	7403.4	0	16.266	*Homo sapiens* aarF domain containing kinase 2 (ADCK2), mRNA.
RIPK2	878.8	0	0	1982.6	0	15.927	*Homo sapiens* receptor-interacting serine-threonine kinase 2 (RIPK2), mRNA.
CPSF1	10642.7	0	0	13781.3	0	15.563	*Homo sapiens* cleavage and polyadenylation specific factor 1, 160kDa (CPSF1), mRNA.
EIF2B2	2521.4	0	0	4360.2	0	15.563	*Homo sapiens* eukaryotic translation initiation factor 2B, subunit 2 beta, 39kDa (EIF2B2), mRNA.
SPP1	2625	0	0	9534.9	0	14.985	*Homo sapiens* secreted phosphoprotein 1 (SPP1), transcript variant 2, mRNA.
SCAMP3	9059.8	0	0	10538.2	0	14.605	*Homo sapiens* secretory carrier membrane protein 3 (SCAMP3), transcript variant 1, mRNA.
GCNT3	349	0	0	3114.7	0	13.795	*Homo sapiens* glucosaminyl (N-acetyl) transferase 3, mucin type (GCNT3), mRNA.
PPM1F	3824.6	0	0	7254.5	0	13.748	*Homo sapiens* protein phosphatase 1F (PP2C domain containing) (PPM1F), mRNA.
GPC3	329.2	0	0	3532.4	0	13.657	*Homo sapiens* glypican 3 (GPC3), mRNA.
EIF2C2	7132	0	0	12596.9	0	13.605	*Homo sapiens* eukaryotic translation initiation factor 2C, 2 (EIF2C2), mRNA.
CUEDC1	130.5	0	0	573.2	0	13.518	*Homo sapiens* CUE domain containing 1 (CUEDC1), mRNA.

Discussion

Formaldehyde reacts with the nucleic acids in several ways. The formation of an N-methylol ($N–CH_2OH$) followed by an electrophilic attack to form a methylene bridge between amino groups was speculated by Srinivasan *et al.* [18]. Masuda *et al.* tried to prove this hypothesis using oligoRNA. We learn from their study that reactivity of the bases decreases in the following order: U<G<A/C, pointing out that the tertiary amino group is the first which is being targeted by formalin [19]. On this basis, McGhee JD and von Hippel PH concluded that the poly(A) tail of mRNA would be strongly modified by fixation. Thus, reverse transcription

would not synthesize the best cDNA due to a non-proper annealing of the oligo(dT) to the poly(A) tail [20].

Another disadvantage for the cDNA synthesis is the degradation of RNA caused by formalin-fixation, meaning that the purified RNA from FFPE tissue might not contain both the poly(A) tail and the target area for PCR amplification [19]. This highly degraded RNA has proved not to be useful in the conventional microarray studies [21]. The Illumina WG-DASL assay kit uses random-priming in the cDNA synthesis step, especially for overcoming the downsides of formalin fixation, any unique regions of the gene being recognized by the probes, without limiting the targeting with optimal probes at the 3' end of the transcripts [6].

Several studies have been carried out in the past years using wide genome DASL assay on a number of different normal and pathological FFPE tissues, including breast, prostate, liver, colon and lung [5, 6, 22, 23].

One of these studies conducted on samples from the colon found that sets of differentially expressed genes identified in FFPE samples resembled those identified from fresh-frozen samples, but with approximately 50% less genes detected in the assay using RNA purified from FFPE tissue [24].

Another study with highly reproducible intensity measurements, which demonstrated that gene expression profiling of RNAs from FFPE samples is possible, was run on prostate, colon, breast, and lung tissue. By using DASL assay and universal microarrays, despite the extensive degradation of the material, they demonstrated that DASL assay combines the advantages of array-based gene expression analysis with those of multi-plexed qPCR [6]. In their data interpretation, the importance of recognizing that the output of the DASL assay reflects the extended and ligated query oligo-nucleotide pool was highlighted. The measurement of gene expression is done indirectly and it depends on the "labeling competition" in the PCR amplification. Thus, changes in hybridization signal may not reflect changes of the number of transcripts in the most accurate way [6].

Hoshida Y *et al.* used RNA extracted from macro-dissected FFPE tissue samples of hepatocellular carcinoma and adjacent liver to run a wide genome DASL assay. They obtained high quality data from samples of 90% of their patients, including the ones that were in storage for more than 24 years [23].

In 2010, Kibriya MG *et al.* conducted a study on breast cancer tissue using WG-DASL assay, and compared the gene expression profile of FFPE and fresh frozen (FF) tissue. Similarities between FFPE and FF samples according to gene ontology classification suggested that FFPE can be successfully used for identifying groups of genes that may be expressed differently in tumors [22].

Our study confirms that gene expression profiling based on the combination of laser microdissection of FFPE tissue and whole genome DASL assay with differential and clustering analysis is feasible. This methodology applies well to the investigation of liver disorders in which different cell sub-populations are in close relationship, due to the particular liver microscopical configuration, diluting and contaminating the RNA yield if whole tissue samples are used for RNA extraction. This methodology is particularly suitable for molecular studies on hepatocellular carcinoma, in view of the characteristic morphological heterogeneity of this tumor including its mixed hepatocellular and cholangiocellular variant.

Conclusions

The whole genome DASL assay can be used on FFPE samples obtained by laser microdissection, despite RNA degradation and chemical modification, giving the opportunity to investigate specific cell populations from archival histological material.

Contribution Note

The first two authors have equally contributed to this work.

References

[1] Thorgeirsson SS, Grisham JW, *Molecular pathogenesis of human hepatocellular carcinoma*, Nat Genet, 2002, 31(4): 339–346.

[2] Lemmer ER, Friedman SL, Llovet JM, *Molecular diagnosis of chronic liver disease and hepatocellular carcinoma: the potential of gene expression profiling*, Semin Liver Dis, 2006, 26(4):373–384.

[3] Maass T, Sfakianakis I, Staib F, Krupp M, Galle PR, Teufel A, *Microarray-based gene expression analysis of hepatocellular carcinoma*, Curr Genomics, 2010, 11(4):261–268.

[4] April C, Klotzle B, Royce T, Wickham-Garcia E, Boyaniwsky T, Izzo J, Cox D, Jones W, Rubio R, Holton K, Matulonis U, Quackenbush J, Fan JB, *Whole-genome gene expression profiling of formalin-fixed, paraffin-embedded tissue samples*, PLoS One, 2009, 4(12):e8162.

[5] Bibikova M, Talantov D, Chudin E, Yeakley JM, Chen J, Doucet D, Wickham E, Atkins D, Barker D, Chee M, Wang Y, Fan JB, *Quantitative gene expression profiling in formalin-fixed, paraffin-embedded tissues using universal bead arrays*, Am J Pathol, 2004, 165(5):1799–1807.

[6] Bibikova M, Yeakley JM, Chudin E, Chen J, Wickham E, Wang-Rodriguez J, Fan JB, *Gene expression profiles in formalin-fixed, paraffin-embedded tissues obtained with a novel assay for microarray analysis*, Clin Chem, 2004, 50(12):2384–2386.

[7] Fan JB, Yeakley JM, Bibikova M, Chudin E, Wickham E, Chen J, Doucet D, Rigault P, Zhang B, Shen R, McBride C, Li HR, Fu XD, Oliphant A, Barker DL, Chee MS, *A versatile assay for high-throughput gene expression profiling on universal array matrices*, Genome Res, 2004, 14(5):878–885.

[8] Blatt R, Srinivasan S, *Defining disease with laser precision: laser capture microdissection in gastroenterology*, Gastro-enterology, 2008, 135(2):364–369.

[9] Tachikawa T, Irié T, *A new molecular biology approach in morphology: basic method and application of laser micro-dissection*, Med Electron Microsc, 2004, 37(2):82–88.

[10] Guedj N, Dargere D, Degos F, Janneau JL, Vidaud D, Belghiti J, Bedossa P, Paradis V, *Global proteomic analysis of microdissected cirrhotic nodules reveals significant biomarkers associated with clonal expansion*, Lab Invest, 2006, 86(9):951–958.

[11] Lashbrook CC, Cai S, *Cell wall remodeling in Arabidopsis stamen abscission zones: temporal aspects of control inferred from transcriptional profiling*, Plant Signal Behav, 2008, 3(9):733–736.

[12] Casson SA, Spencer MW, Lindsey K, *Laser-capture micro-dissection to study global transcriptional changes during plant embryogenesis*, Methods Mol Biol, 2008, 427:111–120.

[13] Montag M, van der Ven K, Delacrétaz G, Rink K, van der Ven H, *Laser-assisted microdissection of the zona pellucida facilitates polar body biopsy*, Fertil Steril, 1998, 69(3):539–542.

[14] Ieta K, Ojima E, Tanaka F, Nakamura Y, Haraguchi N, Mimori K, Inoue H, Kuwano H, Mori M, *Identification of overexpressed genes in hepatocellular carcinoma, with special reference to ubiquitin-conjugating enzyme E2C gene expression*, Int J Cancer, 2007, 121(1):33–38.

[15] Chen L, Yan HX, Yang W, Hu L, Yu LX, Liu Q, Li L, Huang DD, Ding J, Shen F, Zhou WP, Wu MC, Wang HY, *The role of microRNA expression pattern in human intrahepatic cholangiocarcinoma*, J Hepatol, 2009, 50(2):358–369.

[16] Baba N, Kobashi H, Yamamoto K, Terada R, Suzuki T, Hakoda T, Okano N, Shimada N, Fujioka S, Iwasaki Y, Shiratori Y, *Gene expression profiling in biliary epithelial cells of primary biliary cirrhosis using laser capture micro-dissection and cDNA microarray*, Transl Res, 2006, 148(3): 103–113.

[17] Honda M, Yamashita T, Ueda T, Takatori H, Nishino R, Kaneko S, *Different signaling pathways in the livers of patients with chronic hepatitis B or chronic hepatitis C*, Hepatology, 2006, 44(5):1122–1138.

[18] Srinivasan M, Sedmak D, Jewell S, *Effect of fixatives and tissue processing on the content and integrity of nucleic acids*, Am J Pathol, 2002, 161(6):1961–1971.

[19] Masuda N, Ohnishi T, Kawamoto S, Monden M, Okubo K, *Analysis of chemical modification of RNA from formalin-fixed samples and optimization of molecular biology applications for such samples*, Nucleic Acids Res, 1999, 27(22):4436–4443.

[20] McGhee JD, von Hippel PH, *Formaldehyde as a probe of DNA structure. r. Mechanism of the initial reaction of Formaldehyde with DNA*, Biochemistry, 1977, 16(15):3276–3293.

[21] Karsten SL, Van Deerlin VM, Sabatti C, Gill LH, Geschwind DH, *An evaluation of tyramide signal amplification and archived fixed and frozen tissue in microarray gene expression analysis*, Nucleic Acids Res, 2002, 30(2):E4.

[22] Kibriya MG, Jasmine F, Roy S, Paul-Brutus RM, Argos M, Ahsan H, *Analyses and interpretation of whole-genome gene expression from formalin-fixed paraffin-embedded tissue: an illustration with breast cancer tissues*, BMC Genomics, 2010, 11:622.

[23] Hoshida Y, Villanueva A, Kobayashi M, Peix J, Chiang DY, Camargo A, Gupta S, Moore J, Wrobel MJ, Lerner J, Reich M, Chan JA, Glickman JN, Ikeda K, Hashimoto M, Watanabe G, Daidone MG, Roayaie S, Schwartz M, Thung S, Salvesen HB, Gabriel S, Mazzaferro V, Bruix J, Friedman SL, Kumada H, Llovet JM, Golub TR, *Gene expression in fixed tissues and outcome in hepatocellular carcinoma*, N Engl J Med, 2008, 359(19):1995–2004.

Corresponding author

Corina Gabriela Cotoi, Clinical Research Fellow, Liver Histology, Institute of Liver Studies, King's College Hospital, Denmark Hill, London, SE5 9RS, UK; Phone 0044 (0)20 3299 3734, Fax 0044 (0)20 3299 3125, e-mail: corina.cotoi@nhs.net

Received: June 30th, 2012

Accepted: November 25th, 2012